Nitric Oxide 91 (2019) 42–51

Contents lists available at ScienceDirect

Nitric Oxide

journal homepage: www.elsevier.com/locate/yniox

Structure effect of water-soluble iron porphyrins on catalyzing protein tyrosine nitration in the presence of nitrite and hydrogen peroxide

Jiayu Li[a], Zhen Yang[b], Hailing Li[a,**], Zhonghong Gao[a,*]

[a] Hubei Key Laboratory of Bioinorganic Chemistry & Materia Medica, School of Chemistry and Chemical Engineering, Huazhong University of Science & Technology, Wuhan, 430074, PR China

[b] Center for Bioenergetics, Houston Methodist Research Institute, Houston, TX, 77030, United States

ARTICLE INFO

Keywords:
Protein nitration
Water-soluble iron porphyrins
Catalytic activity
Peroxynitrite decomposition
Antioxidation

ABSTRACT

Water-soluble iron porphyrins, such as FeTPPS (5,10,15,20-tetrakis (4-sulfonatophenyl) porphyrinato iron (III)), FeTMPyP (5,10,15,20-tetrakis (N-methyl-4′-pyridyl) porphyrinato iron (III) chloride) and FeTBAP (5,10,15,20-tetrakis (4-benzoic acid) porphyrinato iron (III)), are highly active catalysts for peroxynitrite decomposition and thereby have been suggested as therapeutic agent for inflammatory diseases that implicate the involvement of nitrotyrosine formation. Here, we systemically investigated catalytic properties of FeTPPS, FeTMPyP and FeTBAP on protein nitration in the presence of hydrogen peroxide and nitrite. We showed that FeTPPS, FeTBAP and FeTMPyP all exhibited higher peroxidase activity in compared with hemin. As to protein nitration, the catalytic effect of FeTPPS and FeTBAP are effective in the presence of hydrogen peroxide and nitrite, while negligible BSA nitration was observed in the case of FeTMPyP. Moreover, the underlying mechanism of the oxidation of FeTPPS, FeTBAP and FeTMPyP was further studied. Collectively, our results suggest that, compound I and II species are involved in as the key intermediates in FeTMPyP/H_2O_2 system as similar as those in FeTPPS/H_2O_2 and FeTBAP/H_2O_2 system. As compared to weak antioxidants, TPPS and TBAP, however, TMPyP scavenges oxo-Fe (IV) intermediates of FeTMPyP at a faster rate by significant self-degradation; results in the shortest lifetimes of O=Fe^{IV}-TMPyP and the lowest catalytic activity on oxidizing tyrosine and nitrite; and therefore, attributes to inactivation of FeTMPyP in protein nitration. In addition, association of FeTMPyP to BSA was found weak, while strong binding of FeTPPS and FeTBAP were observed. The weak binding keeps away of target residue of BSA from the center of FeTMPyP where the RNS is generated, which might be attributed as additional factors to the inactivation of FeTMPyP in protein nitration.

1. Introduction

Protein tyrosine nitration is an oxidative post-translational modification that affects protein structure and function and attributes to the pathogenesis of many inflammatory diseases [1–4], such as neurodegenerative disease, cardiovascular disease, and diabetes [3,5–10]. Peroxynitrite-dependent route of nitrotyrosine formation have been well demonstrated in vitro, therefore, the existence of tyrosine nitration in tissues had once been taken as the footprint of peroxynitrite [1,3,4,9]. To antagonize peroxynitrite induced injury, water-soluble iron porphyrin, such as FeTPPS (5,10,15,20-tetrakis (4-sulfonatophenyl) porphyrinato iron (III)), FeTMPyP (5,10,15,20-tetrakis (N-methyl-4′-pyridyl) porphyrinato iron (III) chloride) and FeTBAP (5,10,15,20-tetrakis (4-benzoic acid) porphyrinato iron (III)) (Fig. 1), are receiving increasing attention to function as highly active peroxynitrite decomposition catalysts at physiological pH and temperature [11–15]. Evidences that FeTPPS, FeTMPyP and FeTBAP protect cells from either exogenously introduced or endogenously induced peroxynitrite damage accompanied by a reduction of nitrotyrosine formation have been established in various cellular systems [12,13]. Thus, FeTPPS, FeTMPyP and FeTBAP have been suggested as a unique class of anti-inflammatory agent through reducing nitrotyrosine formation [12–15].

However, under inflammatory conditions, it is most likely that several nitrating pathways operate simultaneously [1,10,16,17], and a preferred mechanism is determined by the presence of inflammatory cells and compartmentalization of the various components of the reaction [1]. For example, hemin (Ferriprotoporphyrin IX chloride) or heme peroxidase/H_2O_2/NO_2^- system is a preferred way to cause protein tyrosine nitration in hemolytic diseases and atherosclerotic plaque,

* Corresponding author.
** Corresponding author.
E-mail addresses: lihailing86@hust.edu.cn (H. Li), zhgao144@hust.edu.cn (Z. Gao).

https://doi.org/10.1016/j.niox.2019.07.007
Received 11 February 2019; Received in revised form 17 July 2019; Accepted 22 July 2019
Available online 24 July 2019
1089-8603/

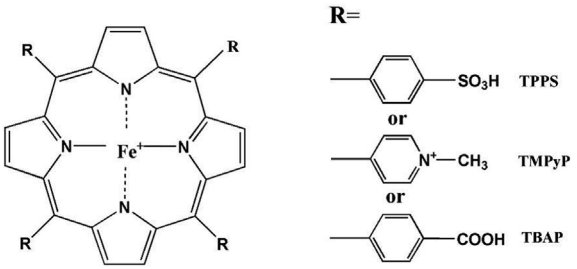

Fig. 1. Chemical structures of iron porphyrins (FeTPPS, FeTMPyP and FeTBAP) and corresponding porphin derivatives (TPPS, TMPyP and TBAP).

due to the abnormal release of free heme and ubiquitous NO_2^- and H_2O_2 [16,18,19]. Recently, we found that FeTPPS, an analogue to hemin, could effectively catalyze protein tyrosine nitration in vitro in the presence of H_2O_2 and NO_2^- [20], which supports previous in vivo result reported by Burgoyne et al. that FeTPPS dramatically enhanced global protein nitration in LPS-treated rats [21]. Hence, it becomes interesting to know whether other hemin water-soluble derivatives, such as FeTMPyP and FeTBAP, possess the similar property. And the finding will surely provide a great contribution in the designing of balanced therapies for pharmacological intervention in peroxynitrite related diseases.

2. Experimental and methods

2.1. Materials

Bovine serum albumin (BSA), rabbit polyclonal antibody against 3-nitrotyrosine (3-NT), 2,2′-azinobis (3-ethylbenzothiazoline-6-sulfonic acid) diammonium salt (ABTS), 3,3′,5,5′-tetramethylbenzidine (TMB) and Ferriprotoporphyrin IX (hemin) were purchased from Sigma. 5,10,15,20-tetrakis (4-sulfonatophenyl) porphyrinato iron (III) (FeTPPS), 5,10,15,20-tetrakis (N-methyl-4′-pyridyl) porphyrinato iron (III) chloride (FeTMPyP), 5,10,15,20-tetrakis (4-benzoic acid) porphyrinato iron (III) (FeTBAP) were purchased from Frontier Scientific Inc. 5,10,15,20-tetrakis-(4-sulfonatophenyl)-porphyrin (TPPS), 5,10,15,20-tetrakis (4-benzoic acid)-porphyrin (TBAP) and 5,10,15,20-tetrakis (N-methyl-4-pyridyl) -porphyrin (TMPyP) were purchased from Shanghai Mackin Biochemical Co, Ltd. Tetrabutylammonium perchlorate were obtained from Aladdin. Horseradish peroxidase-conjugated goat anti-rabbit IgG were purchased from Pierce. All solvents and other reagents were analytical purity and commercially available.

2.2. Measurement of peroxidase activity by UV–Visible method

The peroxidase activity of iron porphyrin was measured by monitoring the increase of TMB oxidation product, which was indicated by its UV–Visible absorbance at 652 nm. The reaction mixtures contained TMB (0.42 mM), iron porphyrin (0.4 μM) and H_2O_2 (3 mM) in citric acid buffer (50 mM, pH 5.0). Reaction was initiated by adding H_2O_2 at 37 °C [22].

Another substrate, ABTS, was also used to assess the peroxidase activity. The measurement was performed by monitoring the increase of ABTS oxidation product indicated by its UV–Visible absorbance at 405 nm. The reaction mixtures contained ABTS (5 mM), iron porphyrin (1 μM) and H_2O_2 (3 mM) in phosphate buffer solution (PBS 100 mM, pH 6.0). Reaction was initiated by adding H_2O_2 at 37 °C [22].

2.3. Detection of BSA nitration by dot blot

Iron porphyrin (hemin, FeTPPS, FeTMPyP or FeTBAP) catalyzed BSA nitration: reaction mixture contained $NaNO_2$ (1 mM), H_2O_2 (1 mM), BSA (1 mg m·L^{-1}) and catalysts (hemin, FeTPPS, FeTMPyP and FeTBAP, 10 μM), in phosphate buffer solution (100 mM, pH 6–8).

Also, effects of porphin derivatives, i.e. TPPS, TMPyP and TBAP on hemin/H_2O_2/NO_2^- induced BSA nitration were examined. The reaction mixtures contained $NaNO_2$ (1 mM), H_2O_2 (1 mM), BSA (1 mg·mL^{-1}), hemin (10 μM) and porphin derivative (10 μM) in phosphate buffer solution (PBS 100 mM, pH 7.4).

Upon completion of the reaction, BSA nitration was detected as the procedure described as followed. The reaction mixture was pre-incubated at 37 °C for 30 min. Then 100 μL reaction mixture was mixed with 25 μL of 5 × loading buffer and heated at 100 °C for 3 min as loading sample. Afterwards, 3 μL loading samples were transferred to nitrocellulose membranes. The nitrocellulose membranes were detected by sequential incubation firstly with a rabbit polyclonal antibody against 3-nitrotyrosine (3-NT) (1:1000) for 2 h and then with horseradish peroxidase-conjugated goat anti-rabbit IgG (1:4000) for 1 h. Chemiluminescence was used to identify specific proteins using the ECL system (Pierce). The density is obtained with gel image system.

2.4. Detection of dityrosine by fluorescence method

The fluorescence spectroscopy (Shimadzu Co., Japan) was adapted to quantify dityrosine as previously described [22]. Dityrosine fluorescence was excited at 325 nm and scanned its emission from 350 to 500 nm with a 5 nm gap width. The fluorescence intensity of dityrosine at 414 nm was recorded every 10 s. Dityrosine formation from L-tyrosine was measured upon the addition of 200 μM H_2O_2 to 200 μM L-tyrosine and 1 μM iron porphyrin in PBS (100 mM, pH 7.4) at room temperature. Reactions were initiated by adding H_2O_2.

2.5. Detection of nitrate by HPLC

The reaction mixtures contained iron porphyrin (10 μM), H_2O_2 (1 mM) and NO_2^- (1 mM) in PBS (100 mM, pH = 7.4). H_2O_2 was used to initiate the reaction. After incubating for 30 min, the reaction mixtures were filtered by 0.22 μm micro-pore filter. Nitrate was quantified by high performance liquid chromatography (HPLC, Agilent, USA) equipped with an ultraviolet diode array spectrophotometer. C18 reverse phase column was used. Solvent A contained 2.5 mM tetrabutylammonium perchlorate, 0.6 mM potassium dihydrogen phosphate (KH_2PO_4) and 0.6 mM disodium hydrogen phosphate (Na_2HPO_4). Solvent B was methanol. The mobile phase consisted of 98% solvent A and 2% solvent B. Column temperature was 25 °C and pump flow rate kept at 1 mL·min^{-1} [23].

2.6. Cyclic voltammetry (CV)

Cyclic voltammograms of FeTPPS, FeTMPyP, FeTBAP, TPPS, TMPyP and TBAP were obtained using a CHI660D electrochemical workstation (shanghai, china). A three-electrode cell system contained a glassy carbon electrode as the working electrode, a saturated calomel electrode as the reference electrode, and a platinum wire as the counter electrode. Prior to each experiment, the glassy carbon electrode was cleaned with alumina polishing power (0.05 μm), sonicated with ethanol for 1.5 min, rinsed with distilled-deionized water, wiped with tissue paper, and immersed in solution containing 40 μM iron porphyrin or 80 μM porphin derivative in 100 mM PBS at pH = 7.4. Control experiments were performed using 100 mM PBS at pH = 7.4. Before each measurement, all solutions were bubbled with nitrogen gas for 20 min to remove oxygen gas dissolved in solution. Scan rate was 10 mV s^{-1}.

2.7. Differential pulse voltammetry (DPV)

Differential pulse voltammograms of 40 μM iron porphyrin (FeTPPS, FeTMPyP and FeTBAP) in 100 mM PBS at pH = 7.4 were recorded using a CHI660D electrochemical workstation (shanghai, china). The electrochemical cell consists of a three-electrode cell with glassy carbon

electrode as the working electrode, a saturated calomel electrode as the reference electrode, and a platinum wire as the counter electrode. DPV parameters were as follows: amplitude 0.025 V; pulse period 0.5 s; and pulse width 0.05 s.

2.8. Detection of oxo-iron (IV) porphyrin by stopped flow method

For this experiment, the spectra of oxo-iron (IV) porphyrin were observed using SX20 Stopped Flow Spectrometer (Applied Photophysics Ltd, UK). Reactions between iron porphyrin and H_2O_2 were single-mixing experiments. After mixing, the solutions consisted of 250 μM H_2O_2 and 5 μM iron porphyrin. The concentration exhibited in the case was the final concentration after mixing.

2.9. Detection of degradation products by ESI-MS

To determine the degradation products, the mixtures were measured with eletro-spray ionization mass spectroscopy (ESI-MS, Agilent). In the presence or absence of NO_2^- (1 mM), iron porphyrin (100 μM) was mixed with H_2O_2 (1 mM) in PBS (100 mM, pH 7.4). After incubating for 30 min at 37 °C, samples were detected with MS. The parameters were as follows: capillary voltage 4.5 kV; iron polarity, negative.

2.10. The binding of iron porphyrin with BSA

UV–Visible spectrophotometer was applied to investigate the reaction of iron porphyrin with BSA. 10 μM FeTPPS, FeTMPyP or FeTBAP was mixed with 30 μM BSA in 100 mM PBS (pH = 7.4) at 37 °C for 15 min.

2.11. Statistical analysis

All data were expressed as the means ± S.D. of three independent experiments. Significance was assessed by using one-way ANOVA ($p < 0.05$ as statistically significant).

3. Results

3.1. The peroxidase activity of iron porphyrins

Two classical substrates, TMB and ABTS were used to evaluate peroxidase activity of FeTPPS, FeTMPyP and FeTBAP. As shown in Fig. 2A, TMB was effectively oxidized by H_2O_2 when hemin, FeTPPS, FeTMPyP or FeTBAP was added. The increased amount of TMB oxidation indicated that the peroxidase activity of FeTMPyP, FeTPPS and FeTBAP are all higher than hemin. This result supports the previous observation by Liu et al. [24] that hemin exhibited the lowest peroxidase activity than FeTPPS and FeTMPyP under oxidation of homovanillic acid with H_2O_2.

The peroxidase activity of iron porphyrins was also analyzed by measuring oxidized ABTS in the presence of H_2O_2 (Fig. 2B). The similar conclusion was obtained. As shown in Fig. 2B, FeTBAP, FeTMPyP and FeTPPS all have the higher peroxidase activity than hemin.

3.2. Iron porphyrin-induced BSA nitration

BSA was nitrated upon exposure to 10 μM hemin, 1 mM H_2O_2 and 1 mM $NaNO_2$ at pH 7.4 (Fig. 3A), which was consistent with previous studies [18,19,25]. As a comparison, similar nitration was also observed upon the catalytic effect of FeTPPS and FeTBAP. However, no nitration was observed in the case of FeTMPyP (Fig. 3A and B).

It has been previously reported that hemin or heme peroxidase-catalyzed BSA nitration in the presence of H_2O_2 and NO_2^- was affected by pH [25,26]. Acidic condition promoted protein tyrosine nitration while basic condition inhibited protein tyrosine nitration. This phenomenon was also found in FeTPPS/H_2O_2/NO_2^- catalyzed BSA nitration [20]. Yang et al. found that the reaction of a water-soluble iron porphyrin complex with H_2O_2 facilitated generation oxo-Fe (IV) porphyrin cation radical at low pH in aqueous solution [27]. Hence, the BSA nitration was also performed at the pH range of 6–8 to examine its pH dependence. As shown in Fig. 3C and D, BSA nitration was noticeably higher in pH lower than 7, in the case of hemin, FeTPPS as well as FeTBAP, the nitration was rapidly decreased as pH increased, which was consistent with previous reports [20,25,26]. On the contrary, no BSA nitration was found when it treated by FeTMPyP in all the tested pH condition (Fig. 3). It becomes interesting to further explore the reasons that FeTMPyP did not effectively catalyze protein nitration as FeTPPS and FeTBAP did, although they all showed high peroxidase activity.

3.3. The mechanism of FeTMPyP in inhibiting BSA nitration

3.3.1. The catalytic activity of FeTMPyP, FeTPPS and FeTBAP on the generation of ·Tyr and ·NO_2

In the presence of H_2O_2, hemin or heme peroxidases are known to catalyze oxidation of tyrosine to form tyrosyl radical (·Tyr), as indicated by the production of the dimerization product dityrosine [10,17,22,28]. Similarly, the formation of dityrosine, which was indicated by its fluorescence exhibited at 414 nm, was monitored to assess the catalytic activity of FeTMPyP, FeTPPS or FeTBAP on the generation of ·Tyr (Fig. 4). It was observed that dityrosine was rapidly formed as soon as the reaction was initiated and reached its maximum at about 100 s after the reaction in both case of FeTPPS and FeTBAP. This result indicated an excellent catalytic activity of FeTPPS and FeTBAP in oxidizing L-tyrosine to tyrosyl radical. However, no dityrosine was observed in the case of FeTMPyP.

A further question is the evolution of NO_2^- in the reaction. In hemin or heme peroxidases/H_2O_2-catalyzed protein nitration, NO_2^- has to be oxidized to NO_2 and then react with ·Tyr to generate

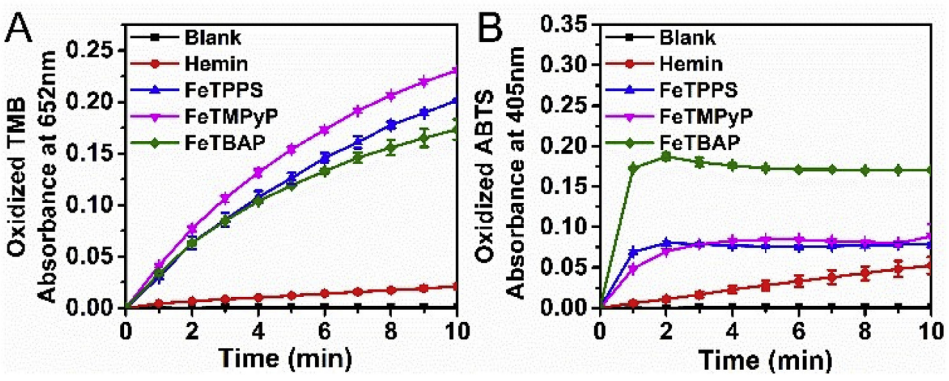

Fig. 2. Peroxidase activity of hemin, FeTPPS, FeTMPyP and FeTBAP. (A) The formation of the oxidized product of TMB was measured by its UV–Visible absorbance at 652 nm. The reaction mixtures contained TMB (0.42 mM), iron porphyrin (0.4 μM) and H_2O_2 (3 mM) in citric acid buffer (50 mM, pH = 5.0). (B) The formation of the oxidized product of ABTS was measured by its UV–Visible absorbance at 405 nm. The reaction mixtures contained ABTS (5 mM), iron porphyrin (1 μM) and H_2O_2 (3 mM) in PBS (100 mM, pH 6.0). Results were presented as means ± S.D. of three independent experiments.

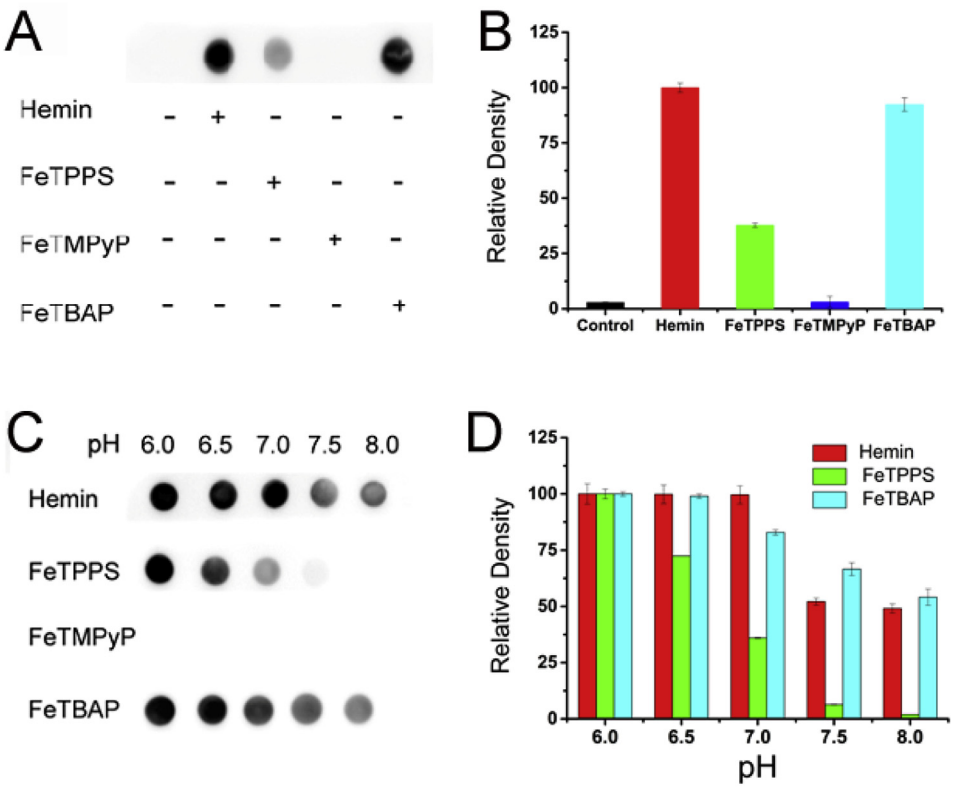

Fig. 3. (A) BSA tyrosine nitration induced by hemin, FeTPPS, FeTMPyP or FeTBAP in the presence of H_2O_2 and NO_2^- at pH 7.4. (B) The densitometric analysis of BSA nitration. All the values were normalized by the hemin control group. (C) pH (6–8) profile of hemin, FeTPPS, FeTMPyP or FeTBAP-catalyzed BSA nitration in the presence of H_2O_2 and NO_2^-. (D) The densitometric analysis of BSA nitration. For hemin at different pHs, all the values were normalized by the hemin control group (hemin at pH 6.0); for FeTPPS at different pHs, all the values were normalized by the FeTPPS control group (FeTPPS at pH 6.0); for FeTBAP at different pHs, all the values were normalized by the FeTBAP control group (FeTBAP at pH 6.0); The reaction mixture contained $NaNO_2$ (1 mM), H_2O_2 (1 mM), BSA (1 mg·mL^{-1}) and iron porphyrin (10 μM) in PBS (100 mM, pH 6–8). Results were presented as means ± S.D. of three independent experiments.

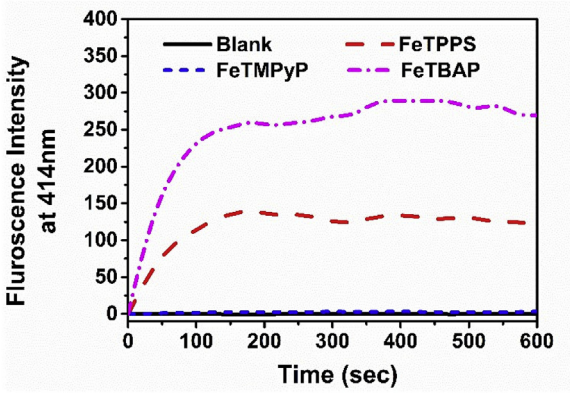

Fig. 4. Kinetics of dityrosine formation in iron porphyrin/H_2O_2/Tyr system. Fluorescence emitted from dityrosine was monitored upon addition of 200 μM H_2O_2 to a solution of 1 μM iron porphyrin and 200 μM L-tyrosine in PBS (100 mM, pH 7.4) at room temperature.

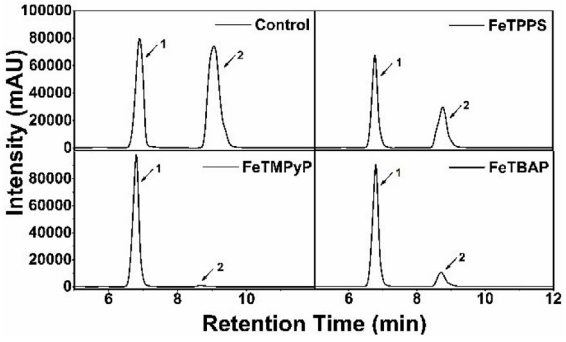

Fig. 5. Detection of nitrate and nitrite by HPLC at 210 nm. Control was standard compounds containing nitrate (1 mM) and nitrite (1 mM); The reaction mixtures contained iron porphyrin (10 μM), H_2O_2 (1 mM) and NO_2^- (1 mM) in PBS (100 mM, pH = 7.4). Peak 1 indicates nitrite, and Peak 2 indicates nitrate.

nitrotyrosine [1,10,17–19]. Meanwhile, the NO_2 will undergo disproportion reaction to form nitrate (NO_3^-) [29,30]. Therefore, measurement of NO_3^- level in the reaction media is an indirect marker to assess the catalytic activity of different iron porphyrin/H_2O_2 systems on the oxidization of NO_2^- to NO_2. And the catalytic activity is essential to trigger the catalytic reaction of protein nitration [17–20]. As shown in Fig. 5, certain amount of NO_3^- was observed in the systems of FeTPPS and FeTBAP. But NO_3^- was barely observed in the FeTMPyP system, indicating that FeTMPyP has the weakest catalytic efficacy in generating NO_2 among these three iron porphyrins.

3.3.2. The intermediates of oxo-iron (IV) porphyrin

Results of Figs. 4 and 5 suggest that the elucidation of the catalytic activity on BSA nitration by heme peroxidase, as well as FeTPPS, FeTMPyP and FeTBAP may depend on understanding their reactive oxo-Fe-(IV) intermediates. Hence, the oxo-Fe-(IV) intermediates in the oxidation of FeTPPS, FeTMPyP or FeTBAP were fully investigated in the further experiments. Firstly, we used two direct electrochemical oxidation methods, namely cyclic voltammetry (CV) (Fig. 6A, C and E) and differential pulse voltammetry (DPV) (Fig. 6B, D and F), to oxidize FeTPPS, FeTMPyP and FeTBAP. Then the stopped-flow method was used to investigate the oxo-Fe-(IV) intermediates generated in the oxidation of FeTPPS, FeTMPyP or FeTBAP by chemical oxidants (H_2O_2) (Fig. 7).

As shown in Fig. 6, similar metal-centered redox behavior was observed in the two distinctive electrochemical analysis. Two separate electro-oxidation peaks (peak 1 and 2) were observed for all FeTPPS, FeTMPyP and FeTBAP, indicating two-step metal redox process [30,32]. The first oxidation wave (peak 1) is proposed as that iron (III) porphyrin (Fe^{III}-Por) undergoes one-electron metal oxidation at 0.94 V for FeTPPS (Figure 7A and B), 0.78 V for FeTMPyP (Figure 6C and D), and 0.88 V for FeTBAP (Fig. 6E and F), to form O=Fe^{IV}-Por species. The second oxidation wave (peak 2) is proposed as one-electron oxidation of O=Fe^{IV}-Por species at 1.15 V for FeTPPS (Figure 6A and B), 1.12 V for

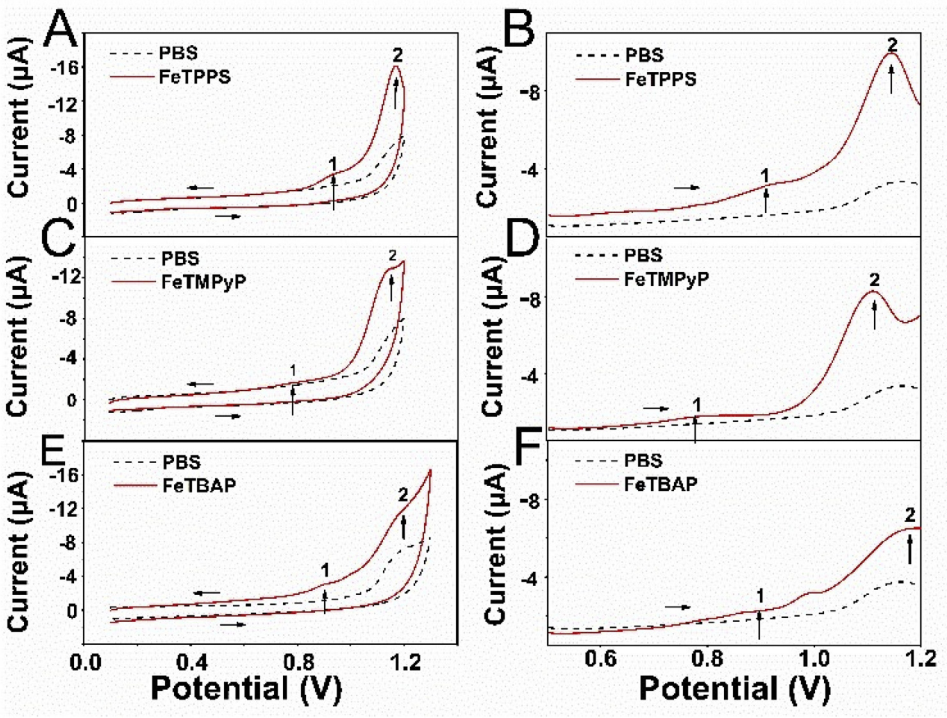

Fig. 6. Cyclic voltammograms of 40 μM FeTPPS (A), FeTMPyP (C) and FeTBPA (E) at a glass carbon electrode in 100 mM PBS at pH = 7.4. Scan rate 10 mV· s^{-1}. Differential pulse voltammograms of 40 μM FeTPPS (B), FeTMPyP (D) and FeTBPA (F) at a glass carbon electrode in 100 mM PBS at pH = 7.4. Pulse amplitude 25 mV and pulse width 50 m s. Control experiments were performed using 100 mM PBS at pH = 7.4. Peak 1 indicates O=Fe^{IV}-Por; Peak 2 indicates O=Fe^{IV}-$Por^{\cdot+}$.

FeTMPyP (Fig. 6C and D), and 1.2 V for FeTBAP (Fig. 6E and F), to form O=Fe^{IV}-$Por^{\cdot+}$. This result supports the previous report by Lei et al. [30], which showed the formation of O=Fe^{IV}-TMPyP and O=Fe^{IV}-$TMPyP^{\cdot+}$ at 0.8 and 1.15 V, respectively, in 50 mM PBS (pH 7.4) using an ITO electrode. In addition, this redox process was similar with a previous study by Trofimova et al. [32], which reported two oxidation waves of MnTMPyP in CV, are corresponding to one-electron redox process to oxo-Mn (IV) and one-electron redox process to oxo-Mn (V), respectively.

Most of non-faradic current is neglected in DPV, therefore, it is more sensitive than classical CV [33]. In this work, close examination of the peak between peak 1 and 2 was performed using DPV (Fig. 6B, D, and F). DPV data showed a broad and un-splitting peak around 0.75 and 0.85 V for FeTMPyP (Fig. 6D), and a splitting peak around 0.95 and 1.03 for FeTBAP (Fig. 6F). It represents the successive oxidation of the porphin derivative by O=Fe^{IV}-$Por^{\cdot+}$ [30]. The oxidation potentials of FeTMPyP and FeTBAP are about 0.8 V and 1.0 V, respectively. It suggests that FeTMPyP is more prone to be oxidized than FeTBAP.

Using stopped-flow method, the generation of two intermediates of FeTPPS, FeTMPyP and FeTBAP oxidized by H_2O_2 were investigated. Upon mixing H_2O_2 with FeTPPS (Fig. 7A), the Soret band of FeTPPS (λ_{max} = 405 nm) shifted to an oxidized iron porphyrin intermediate (λ_{max} = 409 nm) in 5 s without giving any spectral intermediate distinct from the two species. It suggested the conversion of O=Fe^{IV}-$TPPS^{\cdot+}$ (compound I) into O=Fe^{IV}-TPPS (compound II) was accomplished within 5 s. It was consistent with earlier reports that rate constants for compound I (O=Fe^{IV}-$Por^{\cdot+}$) reactions are larger than those of compound II (O=Fe^{IV}-Por) reactions with the same substrate [29,34]. The observed intermediate corresponds to the compound II intermediate (O=Fe^{IV}-TPPS, Soret band at 409 nm (Fig. 7A, insert upper), visible bands at 526 (Fig. 7A, insert below)), which was also consistent with well-studied oxo-Fe (IV) porphyrin intermediates of other water-soluble iron porphyrins [11,35]. This intermediate (compound II, O=Fe^{IV}-TPPS) slowly decayed, but not all restored to FeTPPS (λ_{max} = 405 nm) in 60 s after the reaction (Fig. 7A Insert upper). It suggests the lifetimes of O=Fe^{IV}-TPPS over 60 s. The similar result was observed in the reaction of FeTBAP and H_2O_2 (Fig. 7C). The Soret peak of FeTBAP (λ_{max} = 406 nm) shifted to longer wavelengths (412 nm) in 5 s by the addition of H_2O_2, without giving any spectral intermediate distinct from the two species, indicating that O=Fe^{IV}-TBAP (compound II) as a dominant product appeared (Soret band at 412 nm, visible bands at 520), which is consistent with other heme peroxidase [11,34–36]. Although this intermediate decayed with time, the spectrum of O=Fe^{IV}-TBAP was still observed and persisted over a period of 60 s (Fig. 7C Insert upper). On the contrary, the spectrum of FeTMPyP with H_2O_2 revealed different that the conversion of compound I (O=Fe^{IV}-$TMPyP^{\cdot+}$) into compound II (O=Fe^{IV}-TMPyP), then decayed rapidly back to FeTMPyP (λ_{max} = 419 nm) within 1 s (Fig. 7B). It suggests the shortest lifetime of compound II of FeTMPyP (O=Fe^{IV}-TMPyP) by comparing with O=Fe^{IV}-TPPS and O=Fe^{IV}-TBAP. The short lifetime of O=Fe^{IV}-$TMPyP^{\cdot+}$ (compound I) is consistent with the study by Saha et al. [34], which reported that O=Fe^{IV}-$TMPyP^{\cdot+}$ as an oxidative product of FeTMPyP with H_2O_2, represented nearly 2% of FeTMPyP but it did not accumulate in sufficient concentration to be detected because its decay rate is too fast. The short lifetime of O=Fe^{IV}-TMPyP (compound II) may closely relate to significant destruction of the porphyrin chromophore (bleaching). Notably, only 39% of the FeTMPyP restored in 60 s after the reaction of FeTMPyP with H_2O_2 (Fig. 7B), and the broad and un-slipped peak around 0.8 and 0.95 V represented rapid and successive oxidation of the porphin derivative by O=Fe^{IV}-$TMPyP^{\cdot+}$ (Fig. 6D).

Taken together, these results suggest the short-lived intermediates of FeTMPyP/H_2O_2 is possibly attributed by that its porphin derivative (TMPyP) rapidly scavenges oxo-Fe (IV) intermediates of FeTMPyP by significant self-degradation.

3.3.3. The role of porphin derivative on hemin-induced tyrosine nitration

The total antioxidant capacity of TPPS (Fig. 8A), TMPyP (Fig. 8B) and TBAP (Fig. 8C) were studied by cyclic voltammetry (CV) [37,38]. Two parameters, potential of the anodic peak and area of the anodic peak curve, were used to describe the integrated antioxidant capacity [33,37].

As shown in Fig. 8, the cyclic voltammograms showed an anodic (negative) peak, which corresponds to the total oxidation potential of TPPS, TMPyP and TBAP. Potential of anodic peak was observed at 0.8 V for TPPS, 0.3 V for TMPyP and 0.75 V for TBAP. Correspondingly, the

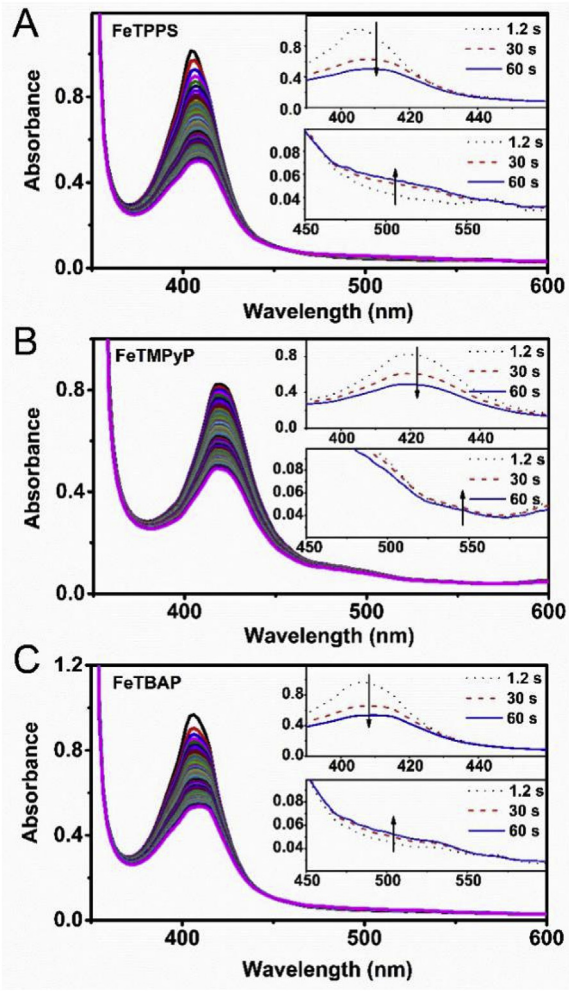

Fig. 7. Rapid-scanning stopped-flow spectra for the reaction of 5 μM FeTPPS (A), FeTMPyP (B) and FeTBAP (C) with 250 μM H_2O_2 in 100 mM PBS at pH = 7.4. Inset: the Soret (inset (upper)) and visible (inset (below)) spectra observed at 1.2, 30 and 60 s.

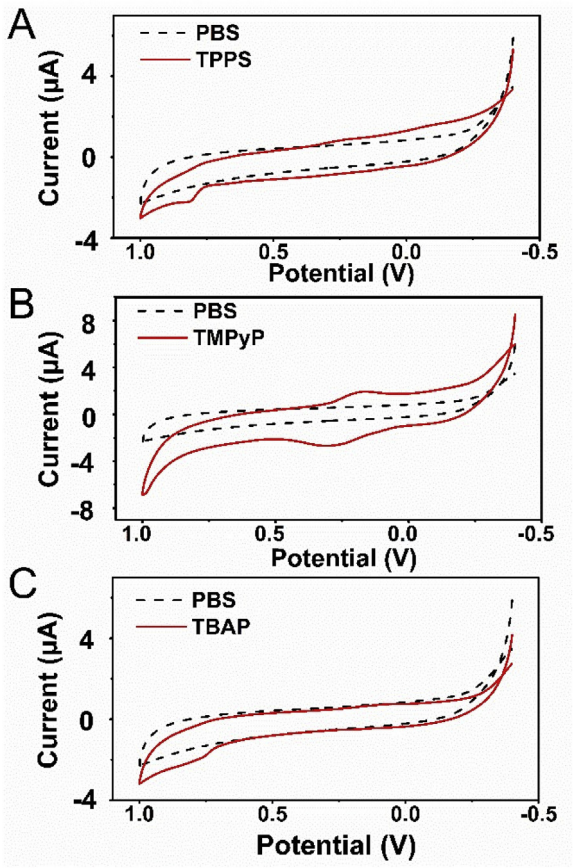

Fig. 8. Cyclic voltammograms of 80 μM TPPS(A), TMPyP (B) and TBAP (C) at scan rate 10 $mV{\cdot}s^{-1}$ in 100 mM PBS at pH = 7.4 by glass carbon electrode. Control experiments were performed using 100 mM PBS at pH = 7.4.

voltammetric peak area was also measured, and it was the largest of TMPyP. Lower potential and larger peak area indicate higher antioxidant activity [33,37–40]. Thus, the potential measured in the CV revealed higher antioxidant activity of TMPyP than that of TPPS and TBAP.

Many reports have demonstrated that antioxidants could effectively inhibit hemin catalyzed tyrosine nitration in the presence of H_2O_2 and NO_2^- [2]. Correspondingly, we also observed the similar inhibitory effect on the hemin-catalyzed tyrosine nitration by the three porphin derivatives (TPPS, TMPyP and TBAP), as shown in Fig. 9. Specifically, TMPyP showed significant inhibitory effect (~75%), whereas inhibitory effect of TPPS and TBAP was only 40% and 20%, respectively (Fig. 9B).

Lente et al. demonstrated that the oxidation products of FeTPPS by H_2O_2 were identified as the iron (III) complex of the biliverdin analogue formed from TPPS and 4-sulfobenzoic acid [41]. Given this report, we systemically investigated the oxidation products in the reaction of iron porphyrin with H_2O_2. Correspondingly, we observed the similar oxidation products characterized by their *m/z* peaks (highlighted by red color in Fig. 10 A, C and E). $C_7H_5O_5S^-$ (*m/z* = 200.9) for FeTPPS; $C_7H_7O_2NCl^-$ (*m/z* = 172) and $C_7H_7ONCl^-$ (*m/z* = 156) for FeTMPyP, and $C_8H_5O_4^-$ (*m/z* = 165) for FeTBAP were found. It indicated that the porphin derivatives, *i.e.* TPPS, TMPyP and TBAP, acted as substrates for iron porphyrin/H_2O_2. However, upon pre-treatment with NO_2^-, it was observed that peaks of the characteristic oxidation products were dramatically reduced (Fig. 10B, D and F), indicating $NO_2^{\cdot}$ as an alternative substrate to be oxidized by oxo-Fe-(IV) [1,10,17–19].

Previously, modification of the heme protein has been reported when HRP was incubated with H_2O_2 and NO_2^- at pH 7, suggesting that NO_2 adds to the heme vinyl groups [42]. However, no nitration product was found in any of FeTPPS (Fig. 10B), FeTMPyP (Fig. 10D) and FeTBAP (Fig. 10F) system by ESI-MS in this work. It indicates that oxidation of NO_2^- by iron porphyrin/H_2O_2 does not result in porphin derivative nitration, that is, TPPS, TMPyP and TBAP do not have NO_2 scavenging capacity.

3.3.4. The binding between iron porphyrin and BSA

It has received increasing attention that hemin bound to the target protein and catalyzed the nitration of neighboring tyrosine residues in the protein, and then affected its function [22,43]. Bathochromic shift and an increased intensity of this band are typical markers that reflect interactions of hemin-Fe with specific amino acid residues of protein matrix [22,44–46].

In the binding assay between BSA and the three iron porphyrins, we saw a shift in the Soret band from 406 nm (FeTPPS) to 417 nm (incubation of FeTPPS and BSA) and an increased intensity of this band (Fig. 11A). These features are indicators of a complex formation between BSA and FeTPPS. Similar result was obtained in FeTBAP. Fig. 11C showed that FeTBAP bound BSA, which is indicated by a clearly red-shift (λ_{max} = 418 nm) and an increased intensity of this band compared with that of free FeTBAP (λ_{max} = 406 nm). However, no bathochromic shift and no increased intensity of band were observed between FeTMPyP and mixture of FeTMPyP with BSA, which showed no bound between FeTMPyP and BSA (Fig. 11B). This result implies the

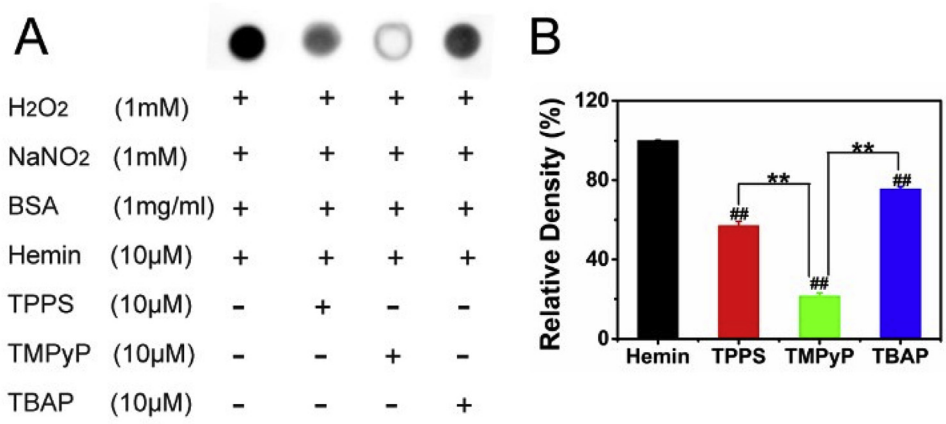

Fig. 9. (A) Effect of porphin derivatives (TPPS, TMPyP or TBAP) on hemin/H_2O_2/NO_2^- induced BSA nitration. (B) The densitometric analysis of BSA nitration. All the values were normalized by the hemin control group; Data was represented as mean ± S. D of three independent experiments. $^{\#\#}p < 0.01$ compared with control value; $^{**}p < 0.01$ compared with TMPyP.

greater distance between the target residue of BSA and the FeTMPyP center where the RNS is generated.

4. Discussion

Water-soluble iron (III) porphyrins, such as FeTPPS, FeTMPyP and FeTBAP, have been demonstrated to possess profound activity in decomposing peroxynitrite and proposed as effective therapeutic agents in peroxynitrite related disease models. The therapeutic effect is believed to operate through reducing protein nitration under condition of inflammation [12,15]. However, it contradicts with the facts that hemin or heme peroxidase/H_2O_2/NO_2^- system is potential to catalyze protein tyrosine nitration, which is a commonly accepted pathway in *vivo* under inflammatory conditions [1,5–10]. In this study, FeTPPS, FeTMPyP and FeTBAP, as hemin analogues, all exhibited excellent peroxidase activity and even higher than the heme (Fig. 2). The high peroxidase activity indicates them as potential catalysts for protein nitration as hemin. In the study of protein nitration, we observed the pronounced BSA nitration by both FeTPPS and FeTBAP in the presence of H_2O_2 and NO_2^-, and the catalytic nitration was revealed pH-dependent (Fig. 3). Interestingly, similar catalytic activity was not observed in the case of FeTMPyP either in acidic condition or basic condition (pH ranging from 6 to 8) (Fig. 3). This unconventional observation prompted us to explore the underlying mechanism that inhibited the catalytic activity of FeTMPyP on protein nitration, and the results might provide an opportunity to develop novel catalysts with the high potential of catalyzing $ONOO^-$ decomposition but with low capability on catalyzing protein nitration in the presence of H_2O_2 and NO_2^-. This kind of compounds could be safer candidates for anti-$ONOO^-$ medicines and more specific indicators for detection of $ONOO^-$ existence in vivo.

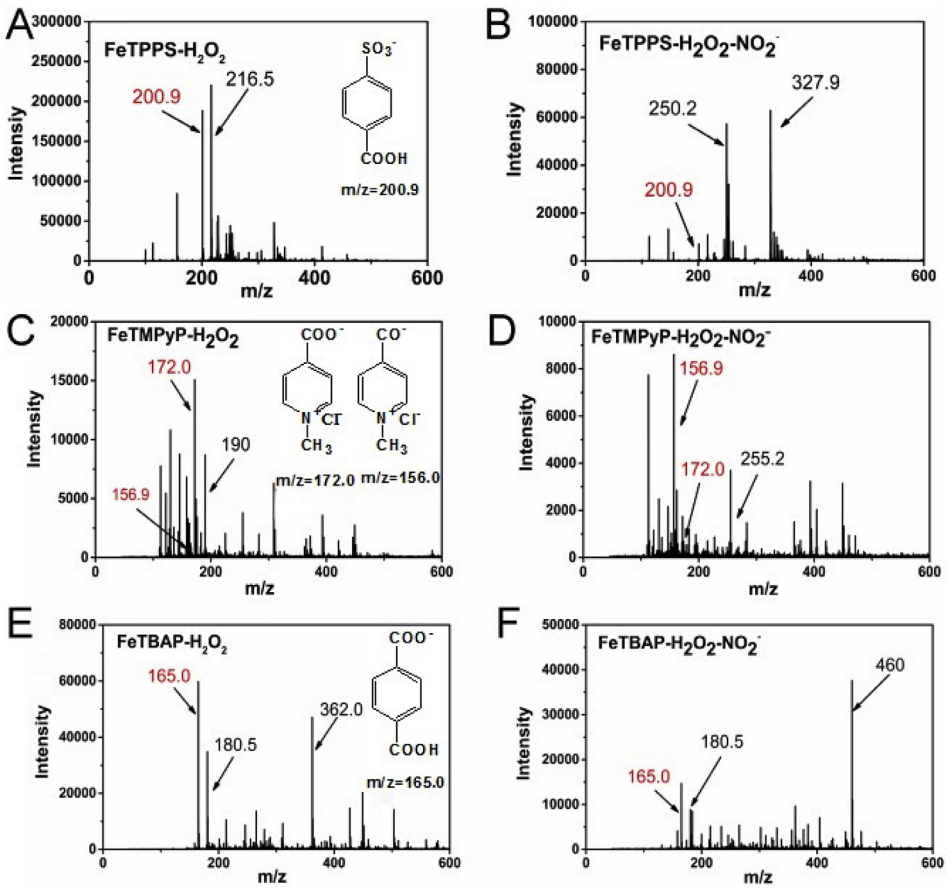

Fig. 10. Measurement of degradation production of iron porphyrin by ESI-MS. Hydrogen peroxide-mediated iron porphyrin decomposition was followed with mass spectrometric analysis in the presence (B, D and F) or absence of NO_2^- (A, C and E). The reaction mixtures contained iron porphyrin (100 μM) and H_2O_2 (1 mM) with or without NO_2^- (1 mM) in PBS (100 mM, pH = 7.4). Inset: the structure of degradation production.

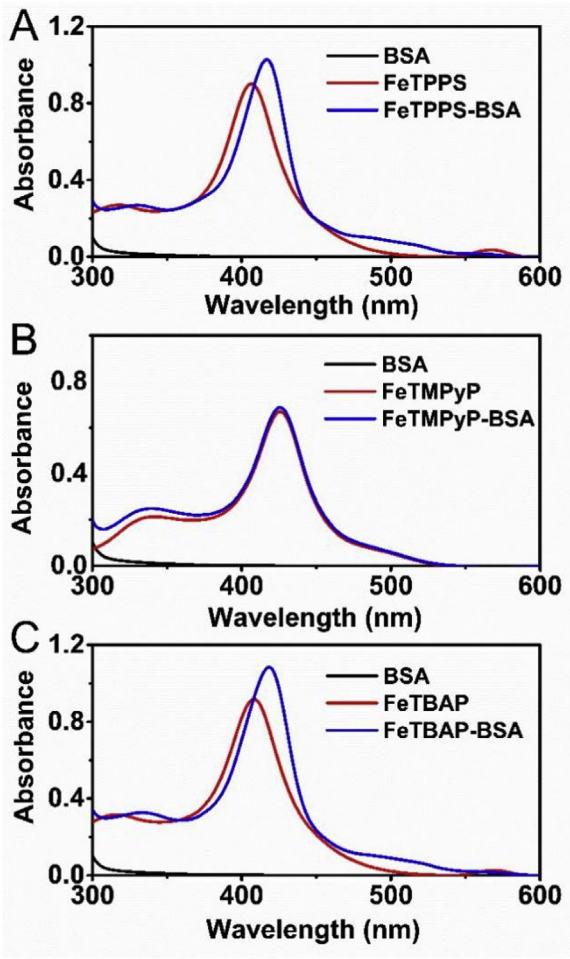

Fig. 11. The binding of FeTPPS (A), FeTMPyP (B) and FeTBAP (C) with BSA. 10 μM iron porphyrin was added into 30 μM BSA in 100 mM PBS (pH = 7.4) and incubated at 37 °C for 15 min for the binding.

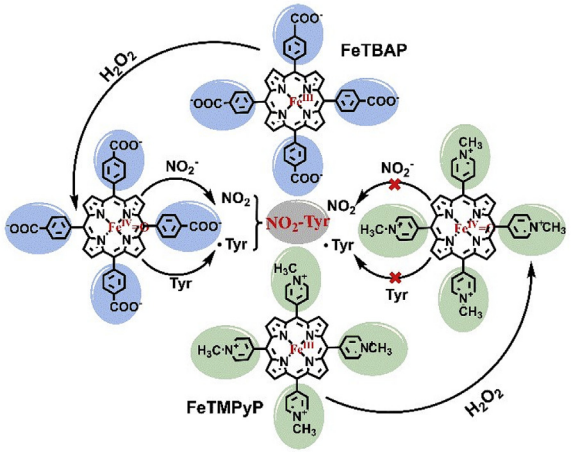

Fig. 12. The modification group of water-soluble iron (III) porphyrin plays an important role in determining its catalytic effect on catalyzing BSA nitration in the presence of H_2O_2 and NO_2^-.

It is known that hemin or heme peroxidase-dependent tyrosine nitration is based on the generation of tyrosyl radicals (·Tyr) and nitrogen dioxide (NO_2) by one-electron reduction of compound I or compound II intermediate in the presence of H_2O_2 and NO_2^- [1,17–19]. Compound I of the heme peroxidase has been described as an oxo-Fe(IV) porphyrin cation radical (O=Fe^{IV}-$Por^{·+}$), while compound II has been described as an oxo-Fe-(IV) species (O=Fe^{IV}-Por). Therefore, the early work established that the catalysis tyrosine nitration normally proceeds via reactions (1)–(4), where A^- is NO_2^- or Tyr, and ·A is $·NO_2$ or ·Tyr.

$$Fe^{III} - Por + H_2O_2 \rightarrow O = Fe^{IV} - Por^{·+} + H_2O \quad (1)$$

$$O = Fe^{IV} - Por^{·+} + A^- \rightarrow O = Fe^{IV} - Por + ·A \quad (2)$$

$$O = Fe^{IV} - Por + A^- + H^+ \rightarrow Fe^{III} - Por + ·A + H_2O \quad (3)$$

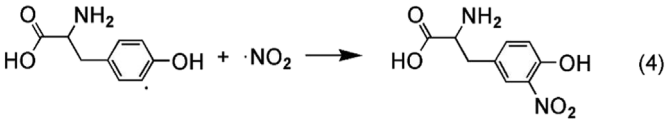

(4)

Compound I : O=Fe^{IV} -$Por^{·+}$ Compound II : O=Fe^{IV} -Por

(4)

Thus, the chain of the catalytic events must start from hemin or heme peroxidase reacting with H_2O_2 to generate high-valency oxo-iron (IV) species, i.e. compound I or compound II [1,17–19]. To unveil the mechanism of FeTPPS, FeTMPyP and FeTBAP on BSA nitration in the presence of H_2O_2 and NO_2^-, we firstly began to identify the reactive intermediates by the direct electrochemical oxidation of FeTPPS, FeTMPyP and FeTBAP using conventional CV and DPV methods (Fig. 6), with a view to avoid possible interference due to excess reactants or secondary products in chemical systems [31]. Both electrochemical techniques gave the similar metal-centered redox behaviors for all FeTPPS, FeTMPyP and FeTBAP, two separate electro-oxidation peaks indicated two-step metal redox process [30], which were speculated as formation of compound II (O=Fe^{IV}-Por) and compound I (O=Fe^{IV}-$Por^{·+}$) intermediates. This result indicates that high-valence oxo-iron (IV) intermediates are involved when these water-soluble iron (III) porphyrins are directly oxidized, which is consistent with well-studied oxo-Fe (IV) porphyrin intermediates of other water-soluble iron porphyrins [27,34,37,42,47]. Furthermore, the reaction of iron porphyrin with H_2O_2 was dynamically monitored using stopped-flow method, in which involvement of compounds I and II intermediates was also suggested (Fig. 7), and compound II was indicated as a dominant product. These results were consistent with the previous observations in heme peroxidase involved oxidation by H_2O_2 [11,34–36]. However, the kinetic scan in the stop-flow method showed a relatively short lifetime of FeTMPyP-induced compound II, which was less than 1 s by comparing to O=Fe^{IV}-TPPS and O=Fe^{IV}-TBAP that persisted over a period of 60 s (Fig. 7). Activity of oxo-Fe (IV) intermediates is very important in the catalytic cycle [1,17,19]. We found that FeTMPyP/HSO_5^-/NO_2^- induced BSA nitration can be observed (Support Information, Fig. S1), because the activity and concentration of oxo-Fe (IV) intermediates from HSO_5^- oxidation is higher than that from H_2O_2 as oxidant [41]. For this reason, we speculated that the weakest catalytic activity of FeTMPyP/H_2O_2 in oxidizing L-tyrosine to ·Tyr (Fig. 4) and NO_2^- to NO_2 (Fig. 5) can be attributed to shorter lifetime of O=Fe^{IV}-TMPyP, which results in FeTMPyP lacking the ability to catalyze BSA nitration in the presence of H_2O_2 and NO_2^- (Fig. 3).

Due to the rather short-lived nature of most nitrating species, it is conceivable that the site of generation of a nitrating agent with respect to the target protein plays a role in determining which proteins become nitrated and possibly also in defining the primary nitration sites [1,43]. In several disease models, nitrated proteins have been detected at the site of injury or within specific cell types, which are known to generate nitrating species [1]. We also observed that FeTMPyP showed no bound with BSA protein while a strong binding was indicated between BSA and the other two iron porphyrins, FeTPPS and FeTBAP (Fig. 11). The fluorescence quenching experiment also demonstrated that FeTMPyP exhibited a very weak association with BSA (K_b $2.3 \times 10^3\ M^{-1}$). However, the binding constants of FeTPPS and FeTBAP were $2.8 \times 10^7\ M^{-1}$ and $3.5 \times 10^7\ M^{-1}$, respectively (Support Information, Fig. S2), which are of the same order of magnitude as that of heme to

human albumin (K_b $7.9 \times 10^7\ M^{-1}$) [44]. Therefore, the greater distance between the target residue of BSA and the FeTMPyP center where the RNS is generated, may be another possible reason for FeTMPyP lacking the ability to catalyze BSA nitration in the presence of H_2O_2 and NO_2^-.

The unstable compound II and unbound with targeted protein seemed attributed to the weak catalytic activity of FeTMPyP on protein nitration. However, it remained unclear how the relatively short lifetime of FeTMPyP-induced compound II was achieved. There was an interesting report from Lente et al. that the oxidized product of FeTPPS by H_2O_2 was found to be the collapse of porphin derivative. It suggested the porphin derivative of FeTPPS, TPPS, as a substrate that was oxidized by the oxo-Fe (IV) intermediates in the reaction [41]. This phenomenon was also observed when FeTPPS, FeTMPyP or FeTBAP was mixed with H_2O_2. The Soret band of the iron porphyrin disappears quickly (Support Information, Fig. S3 (A)), and the Soret band of FeTMPyP disappears more quickly than that of FeTPPS and FeTBAP (Fig. 7). In the presence of NO_2^-, the Soret band of the iron porphyrin decayed slower in all tested iron porphyrins (Support Information, Fig. S3 (B and C)), suggesting that NO_2^- competed with corresponding porphin derivative (TPPS, TMPyP or TBAP) for oxidation by iron porphyrin/H_2O_2. Given these evidences, we speculated that the lower stability of intermediates of FeTMPyP may be partially attributed to the electrochemical capacity of its porphin derivative (TMPyP). It rapidly reduced high-valence oxo-iron (IV) intermediates; inhibited NO_2^- or tyrosine oxidation; and thereby, resulted in negligible BSA nitration in FeTMPyP/H_2O_2/NO_2^- system.

Blasco et al. distinguished antioxidants with high ($E \leq 0.3$ V) and medium power ($E = 0.5$ V) [39]. According to this criterion, Fig. 8 result suggested that TMPyP possessed stronger antioxidant capacity ($E = 0.3$ V) by comparing with TPPS ($E = 0.8$ V) and TBAP ($E = 0.75$ V). By using dot blot, we also clearly demonstrated that TMPyP exhibited higher capacity in competitive inhibiting NO_2^- and tyrosine oxidation by hemin/H_2O_2/NO_2^- (Fig. 9). Moreover, oxidized products from porphin derivatives were also found in the reaction of iron porphyrin with H_2O_2 (Fig. 10). These results suggested that TMPyP reacted easily with oxo-Fe (IV), and the fast reaction of TMPyP with the oxo-Fe (IV) intermediate accounted for the short lifetime of oxo-Fe (IV) intermediate in the FeTMPyP oxidation reaction. The competition reaction of TMPyP surely inhibited oxidation of tyrosine and NO_2^- and thus dramatically reduced the protein nitration. Worth noting is that the proximity of porphin derivative to the site generating the nitrating species (NO_2) may scavenges NO_2 by competitive nitrating porphin derivative [36], which might be another possible mechanism for the antioxidative activity of TMPyP in inactivating FeTMPyP induced BSA nitration. In the presence of H_2O_2 and NO_2^-, the oxidation products for porphin derivatives were found (Fig. 10), but no nitrated ligand products were found in any of FeTPPS, FeTMPyP and FeTBAP system (Fig. 10B, D, and F). These results indicated that inhibiting tyrosine nitration of FeTMPyP was not realized through direct scavenging NO_2 by its ligand (TMPyP) (Fig. 10D), but operated by oxidizing its porphin derivative to irreversibly destructive products, such as $C_7H_7O_2NCl^-$ ($m/z = 172$) and $C_7H_7ONCl^-$ ($m/z = 156$) (Fig. 10C).

At mildly acidic pH, NO_2^- directly reacts with H_2O_2 to form peroxynitrous acid (ONOOH), which causes aromatic nitration [48]. Several reports also suggested that both the classical peroxidase pathway and peroxynitrite mechanism are operative in hemin or heme peroxidase-dependent nitration system [49,50]. However, our result showed no peroxynitrite formation in mixtures of H_2O_2 (1 mM) and NO_2^- (1 mM) in PBS (100 mM, pH = 7.4) (Support Information, Fig. S4), indicating that inactivation FeTMPyP-induced BSA nitration in the presence of H_2O_2 and NO_2^- under the experimental condition must not be ascribed to that FeTMPyP acting as a highly active peroxynitrite decomposition catalyst.

5. Conclusion

We showed that the three water-soluble iron porphyrins, FeTPPS, FeTBAP and FeTMPyP as analogues to hemin, all exhibited excellent peroxidase activity and even higher compared with hemin. In the presence of H_2O_2 and NO_2^-, mechanism of the water-soluble iron (III) porphyrin-dependent tyrosine nitration is similar as that of hemin or heme peroxidase-dependent, and compound I and compound II species are involved in as the key intermediates. However, FeTMPyP seemed no effect on catalyzing protein nitration while the other two analogues, FeTPPS and FeTBAP, preserved the conventional catalytic activity of heme peroxidase on protein nitration (Fig. 12). Further study on the underlying mechanism revealed a different reaction behavior of FeTMPyP in the protein nitration in the comparison with FeTPPS and FeTBAP. Generally, FeTMPyP inactivation on catalyzing protein tyrosine nitration in this system can be mainly attributed to the activity of its porphin derivative, TMPyP, which reacted strongly with the oxo-Fe (IV) intermediate of FeTMPyP that resulted in short lifetime of the intermediates. As TMPyP competes strongly with tyrosine and NO_2^- in the oxidation reaction, oxidized tyrosine and NO_2^- was dramatically inhibited, leading to the pronounced reduction of final protein nitration. Besides, the greater distance between the target residue of BSA and the FeTMPyP center (Fig. 11 and Support Information, Fig. S2) further blocks the possible formation of nitrotyrosine (due to the facts that FeTMPyP/HSO_5/NO_2^- induced BSA nitration can be observed, in Support Information, Fig. S1), which is a minor factor on FeTMPyP inactivation. Finally, FeTMPyP failed in catalyzing protein tyrosine nitration described here must not be attributed to TMPyP as NO_2 scavenger (Fig. 10D) or FeTMPyP is a highly active peroxynitrite decomposition catalyst (Support Information, Fig. S4). Since a better peroxynitrite decomposition catalyst should be with lower capacity in catalyzing protein tyrosine nitration in the presence of H_2O_2 and NO_2^-, the dissection of the mechanism of FeTMPyP inactivation on catalyzing protein tyrosine nitration, in the presence of H_2O_2 and NO_2^-, may provide an instructive model for designing of balanced compounds for pharmacological intervention in peroxynitrite related diseases.

Conflicts of interest

The authors declare no competing financial interest.

Acknowledgment

This work was supported by grants from the National Natural Science Foundation of China (Nos. 31570810, 31770866) and Natural Science Foundation of Hubei Scientific Committee (2016CFA001) and the Fundamental Research Funds for the Central Universities of China (2017KFYXJJ167).

Appendix A. Supplementary data

Supplementary data to this article can be found online at https://doi.org/10.1016/j.niox.2019.07.007.

References

[1] N. Abello, H.A.M. Kerstjens, D.S. Postma, R. Bischoff, Protein tyrosine nitration: selectivity, physicochemical and biological consequences, denitration, and proteomics methods for the identification of tyrosine-nitrated proteins, J. Proteome Res. 8 (2009) 3222–3238.

[2] Y. Zhao, Z. Gao, H. Li, H. Xu, Hemin/nitrite/H_2O_2 induces brain homogenate oxidation and nitration: effects of some flavonoids, Biochim. Biophys. Acta 1675 (2004) 105–112.

[3] S. Hafez, M. Abdelsaid, S.C. Fagan, A. Ergul, Peroxynitrite-induced tyrosine nitration contributes to matrix metalloprotease-3 activation: relevance to hyperglycemic ischemic brain injury and tissue plasminogen activator, Neurochem. Res. 43 (2018) 259–266.

[4] G. Degendorfer, C.Y. Chuang, H. Kawasaki, A. Hammer, E. Malle, F. Yamakura,

M.J. Davies, Peroxynitrite-mediated oxidation of plasma fibronectin, Free Radical Biol. Med. 97 (2016) 602–615.
[5] I.V. Turko, F. Murad, Protein nitration in cardiovascular diseases, Pharmacol. Rev. 54 (2002) 619–634.
[6] G. Peluffo, R. Radi, Biochemistry of protein tyrosine nitration in cardiovascular pathology, Cardiovasc. Res. 75 (2007) 291–302.
[7] N. Lu, X. Li, J. Li, W. Xu, H. Li, Z. Gao, Nitrative and oxidative modifications of enolase are associated with iron in iron-overload rats and in vitro, J. Biol. Inorg. Chem. 16 (2011) 481–490.
[8] X. Li, H. Li, N. Lu, Y. Feng, Y. Huang, Z. Gao, Iron increases liver injury through oxidative/nitrative stress in diabetic rats: involvement of nitrotyrosination of glucokinase, Biochimie 94 (2012) 2620–2627.
[9] P. Pacher, J.S. Beckman, L. Liaudet, Nitric oxide and peroxynitrite in health and disease, Physiol. Rev. 87 (2007) 315–424 87.
[10] A. vanderVliet, J.P. Eiserich, B. Halliwell, C.E. Cross, Formation of reactive nitrogen species during peroxidase-catalyzed oxidation of nitrite - a potential additional, mechanism of nitric oxide-dependent toxicity, J. Biol. Chem. 272 (1997) 7617–7625.
[11] M.K. Stern, M.P. Jensen, K. Kramer, Peroxynitrite decomposition catalysts, J. Am. Chem. Soc. 118 (1996) 8735–8736.
[12] T.P. Misko, M.K. Highkin, A.W. Veenhuizen, P.T. Manning, M.K. Stern, M.G. Currie, D. Salvemini, Characterization of the cytoprotective action of peroxynitrite decomposition catalysts, J. Biol. Chem. 273 (1998) 15646–15653.
[13] S.S. Klassen, S.W. Rabkin, The metalloporphyrin FeTPPS but not by cyclosporin A antagonizes the interaction of peroxynitrate and hydrogen peroxide on cardiomyocyte cell death, Naunyn-Schmiedeberg's Arch. Pharmacol. 379 (2009) 149–161.
[14] G. Bruschetta, D. Impellizzeri, M. Campolo, G. Casili, R. Di Paola, I. Paterniti, E. Esposito, S. Cuzzocrea, FeTPPS reduces secondary damage and improves neurobehavioral functions after traumatic brain injury, Front. Neurosci. 11 (2017) 6.
[15] D. Salvemini, Z.Q. Wang, M.K. Stern, M.G. Currie, T.P. Misko, Peroxynitrite decomposition catalysts: therapeutics for peroxynitrite-mediated pathology, Proc. Natl. Acad. Sci. U.S.A. 95 (1998) 2659–2663.
[16] B. Halliwell, What nitrates tyrosine? Is nitrotyrosine specific as a biomarker of peroxynitrite formation in vivo? FEBS Lett. 411 (1997) 157–160.
[17] N. Campolo, S. Bartesaghi, R. Radi, Metal-catalyzed protein tyrosine nitration in biological systems, Redox Rep. 19 (2014) 221–231.
[18] D.D. Thomas, M.G. Espey, M.P. Vitek, K.M. Miranda, D.A. Wink, Protein nitration is mediated by heme and free metals through Fenton-type chemistry: an alternative to the NO/O_2^- reaction, Proc. Natl. Acad. Sci. U.S.A. 99 (2002) 12691–12696.
[19] K. Bian, Z. Gao, N. Weisbrodt, F. Murad, The nature of heme/iron-induced protein tyrosine nitration, Proc. Natl. Acad. Sci. U.S.A. 100 (2003) 5712–5717.
[20] P.F. Zhang, L. Ma, Z. Yang, H. Li, Z. Gao, 5,10,15,20-Tetrakis(4-sulfonatophenyl) porphyrinato iron(III) chloride (FeTPPS), a peroxynitrite decomposition catalyst, catalyzes protein tyrosine nitration in the presence of hydrogen peroxide and nitrite, J. Inorg. Biochem. 183 (2018) 9–17.
[21] J.R. Burgoyne, O. Rudyk, M. Mayr, P. Eaton, Nitrosative protein oxidation is modulated during early endotoxemia, Nitric Oxide 25 (2011) 118–124.
[22] Y. Huang, Z. Yang, H. Xu, P. Zhang, Z. Gao, H. Li, Insulin enhances the peroxidase activity of heme by forming heme-insulin complex: relevance to type 2 diabetes mellitus, Int. J. Biol. Macromol. 102 (2017) 1009–1015.
[23] H. Xu, Z. Yang, H. Li, Z. Gao, Hemin-graphene derivatives with increased peroxidase activities restrain protein tyrosine nitration, Chem. Eur J. 23 (2017) 17755–17763.
[24] J. Liu, X. Li, Z. Guo, Y. Li, A. Huang, W. Chang, Comparative study on heme-containing enzyme-like catalytic activities of water-soluble metalloporphyrins, J. Mol. Catal. A Chem. 179 (2002) 27–33.
[25] P. Gao, Y. Song, H. Li, Z. Gao, Efficiency of methemoglobin, hemin and ferric citrate in catalyzing protein tyrosine nitration, protein oxidation and lipid peroxidation in a bovine serum albumin-liposome system: influence of pH, J. Inorg. Biochem. 103 (2009) 783–790.
[26] Y. Kambayashi, Y. Hitomi, N. Kodama, M. Kubo, J. Okuda, K. Takemoto, M. Shibamori, T. Takigawa, K. Ogino, pH profile of cytochrome c-catalyzed tyrosine nitration, Acta Biochim. Pol. 53 (2006) 577–584.
[27] S.J. Yang, W. Nam, Water-soluble iron porphyrin complex-catalyzed epoxidation of olefins with hydrogen peroxide and tert-butyl hydroperoxide in aqueous solution, Inorg. Chem. 37 (1998) 606–607.
[28] A. Höhn, T. Jung, T. Grune, Pathophysiological importance of aggregated damaged proteins, Free Radical Biol. Med. 71 (2014) 70–89.
[29] A. Samuni, E. Maimon, S. Goldstein, Mechanism of HRP-catalyzed nitrite oxidation by H_2O_2 revisited: effect of nitroxides on enzyme inactivation and its catalytic activity, Free Radical Biol. Med. 108 (2017) 832–839.
[30] J. Lei, H. Ju, O. Ikeda, Catalytic oxidation of nitric oxide and nitrite mediated by water-soluble high-valent iron porphyrins at an ITO electrode, J. Electroanal. Chem. 567 (2004) 331–338.
[31] S. Rana, K. Tamagake, Formation of ferryl porphyrin by electrochemical reduction of iron porphyrin in aqueous solution, J. Electroanal. Chem. 581 (2005) 145–152.
[32] N.S. Trofimova, A.Y. Safronov, O. Ikeda, Electrochemical and spectral studies on the catalytic oxidation of nitric oxide and nitrite by high-valent manganese porphyrins at an ITO electrode, Electrochim. Acta 50 (2005) 4637–4644.
[33] B.K. Glod, I. Kiersztyn, P. Piszcz, Total antioxidant potential assay with cyclic voltammetry and/or differential pulse voltammetry measurements, J. Electroanal. Chem. 719 (2014) 24–29.
[34] T.K. Saha, S. Karmaker, K. Tamagake, Transient formation of the oxo-iron(IV) porphyrin radical cation during the reaction of iron(III) tetrakis-5,10,15,20-(N-methyl-4-pyridyl) porphyrin with hydrogen peroxide in aqueous solution, Luminescence 18 (2003) 162–172.
[35] J.B. Lee, J.A. Hunt, J.T. Groves, Mechanisms of iron porphyrin reactions with peroxynitrite, J. Am. Chem. Soc. 120 (1998) 7493–7501.
[36] R. Roncone, M. Barbieri, E. Monzani, L. Casella, Reactive nitrogen species generated by heme proteins: mechanism of formation and targets, Coord. Chem. Rev. 250 (2006) 1286–1293.
[37] M.J. Jara-Palacios, M.L. Escudero-Gilete, J.M. Hernandez-Hierro, F.J. Heredia, D. Hernanz, Cyclic voltammetry to evaluate the antioxidant potential in winemaking by-products, Talanta 165 (2017) 211–215.
[38] S. Chevion, M.A. Roberts, M. Chevion, The use of cyclic voltammetry for the evaluation of antioxidant capacity, Free Radical Biol. Med. 28 (2000) 860–870.
[39] A.J. Blasco, M.C. Rogerio, M.C. Gonzalez, A. Escarpa, Electrochemical Index" as a screening method to determine "total polyphenolics" in foods: a proposal, Anal. Chim. Acta 539 (2005) 237–244.
[40] L.M. Magalhaes, M.A. Segundo, S. Reis, J.L.F.C. Lima, Methodological aspects about in vitro evaluation of antioxidant properties, Anal. Chim. Acta 613 (2008) 1–19.
[41] G. Lente, I. Fabian, Kinetics and mechanism of the oxidation of water soluble porphyrin Fe^{III} TPPS with hydrogen peroxide and the peroxomonosulfate ion, Dalton Trans. (2007) 4268–4275.
[42] G. Wojciechowski, P.R.O. de Montellano, Radical energies and the regiochemistry of addition to heme groups. Methylperoxy and nitrite radical additions to the heme of horseradish peroxidase, J. Am. Chem. Soc. 129 (2007) 1663–1672.
[43] H. Ye, Z. Yang, H. Li, Z. Gao, NPY binds with heme to form a NPY-heme complex: enhancing peroxidase activity in free heme and promoting NPY nitration and inactivation, Dalton Trans. 46 (2017) 10315–10323.
[44] E. Karnaukhova, S.S. Krupnikova, M. Rajabi, A.I. Alayash, Heme binding to human alpha-1 proteinase inhibitor, Biochim. Biophys. Acta 1820 (2012) 2020–2029.
[45] K. Hayasaka, K. Kitanishi, J. Igarashi, T. Shimizu, Heme-binding characteristics of the isolated PAS-B domain of mouse Per 2, a transcriptional regulatory factor associated with circadian rhythms, Biochim. Biophys. Acta 1814 (2011) 326–333.
[46] S. Mukherjee, S.G. Dey, Heme Bound Amylin: spectroscopic characterization, reactivity, and relevance to type 2 diabetes, Inorg. Chem. 52 (2013) 5226–5235.
[47] N.G. Giri, S.M.S. Chauhan, Oxidation of polycyclic aromatic hydrocarbons with hydrogen peroxide catalyzed by Iron(III)porphyrins, Catal. Commun. 10 (2009) 383–387.
[48] A. Vandervliet, J.P. Eiserich, C.A. Oneill, B. Halliwell, C.E. Cross, Tyrosine modification by reactive nitrogen species: a closer look, Arch. Biochem. Biophys. 319 (1995) 341–349.
[49] L. Casella, E. Monzani, R. Roncone, S. Nicolis, A. Sala, A. De Riso, Formation of reactive nitrogen species at biologic heme centers: a potential mechanism of nitric oxide-dependent toxicity, Environ. Health Perspect. 110 (2002) 709–711.
[50] R. Floris, S.R. Piersma, G. Yang, P. Jones, R. Wever, Interaction of myeloperoxidase with peroxynitrite: a comparison with lactoperoxidase, horseradish peroxidase and catalase, Eur. J. Biochem. 215 (1993) 767–775.